

Electric Monopole Transition Strengths in ^{62}Ni

L. J. Evitts^{1,2,a}, A. B. Garnsworthy¹, T. Kibédi³, M. Moukaddam¹, B. Alshahrani^{3,4}, T. K. Eriksen³, J. D. Holt¹, S. S. Hota³, G. J. Lane³, B. Q. Lee³, B. P. McCormick³, N. Palalani³, M. W. Reed³, S. R. Stroberg¹, and A. E. Stuchbery³

¹TRIUMF, 4004 Wesbrook Mall, Vancouver BC, V6T 2A3, Canada

²Department of Physics, University of Surrey, Guildford, GU2 7XH, United Kingdom

³Department of Nuclear Physics, Research School of Physics and Engineering, The Australian National University, Canberra, ACT 2601, Australia

⁴King Khaled University, Abha, Kingdom of Saudi Arabia

Abstract. Excited states in ^{62}Ni were populated with a (p, p') reaction using the 14UD Pelletron accelerator at the Australian National University. Electric monopole transition strengths, $\rho^2(E0)$, were measured through simultaneous detection of the internal conversion electrons and γ rays emitted from the de-excitation of populated states, using the Super-e spectrometer coupled with a germanium detector. The strength of the 0_2^+ to 0_1^+ transition has been measured to be $77_{-34}^{+23} \times 10^{-3}$ and agrees with previously reported values. Upper limits have been placed on the 0_3^+ to 0_1^+ and 0_3^+ to 0_2^+ transitions. The measured $\rho^2(E0)$ value of the 2_2^+ to 2_1^+ transition in ^{62}Ni has been measured for the first time and found to be one of the largest $\rho^2(E0)$ values measured to date in nuclei heavier than Ca. The low-lying states of ^{62}Ni have previously been classified as one- and two-phonon vibrational states based on level energies. The measured electric quadrupole transition strengths are consistent with this interpretation. However as electric monopole transitions are forbidden between states which differ by one phonon number, the simple harmonic quadrupole vibrational picture is not sufficient to explain the large $\rho^2(E0)$ value for the 2_2^+ to 2_1^+ transition.

1 Introduction

Electric monopole ($E0$) transitions occur between nuclear states in the same nucleus that possess the same spin and parity, J^π . Due to conservation of angular momentum, single γ -ray emission is forbidden between states of $J^\pi = 0^+$ but the transition can occur via internal conversion electrons and pair production. The strength of $E0$ transitions, $\rho^2(E0)$, is a good indication of the underlying nuclear structure. For example, they provide information that can indicate a change in the nuclear shape or on the mixing between a number of states [1, 2].

For the stable even-even Ni isotopes, $\rho^2(E0)$ values for transitions between 0^+ states have been measured in $^{58,60,62}\text{Ni}$ [3–5] while no measurement exists for ^{64}Ni . Furthermore, $\rho^2(E0 : J^+ \rightarrow J^+)$ values for non-zero spin states have not been measured in the Ni isotopes. The previous measurements are shown in Fig. 1.

It has long been considered that ^{62}Ni is a good example of a quadrupole spherical vibrator due to the 0^+ , 2^+ , 4^+ triplet of states at twice the energy of the 2_1^+ state. The model is further supported by the measurement of a small quadrupole moment, $Q(2_1^+) = +0.05(12)\text{b}$ [6], and the collective $B(E2)$ values [7, 8]. However, the spherical vibrator model has faced challenges in recent years

e.g., Garrett *et al.* have suggested the breakdown of vibrational excitations in the Cd isotopes [9, 10]. In the Cd case it seems that mixing with multi-quasiparticle intruder configurations are likely to play a significant role in the development of apparent collectivity in the ground-state structure.

Chakraborty *et al.* [8] measured the $B(E2 \downarrow : 2_1^+ \rightarrow 0_1^+)$ value in ^{62}Ni to be 12.1(4) W.u., which is in excellent agreement with a theoretical value of 12 W.u. from the vibrator model. However, they also measured the $B(E2 \downarrow : 2_2^+ \rightarrow 2_1^+)$ value for the transition between the suspected two-phonon and one-phonon states to be $12.5_{-3.2}^{+3.8}$ W.u., which is 3σ away from the expected theoretical value based on a spherical quadrupole vibrator of 24 W.u.. A detailed examination of the electric monopole transition strengths is expected to help clarify our understanding of the underlying nature of these excitations.

Various models can be employed to make predictions of electric monopole transition strengths. In the spherical vibrator model the $2_2^+ \rightarrow 2_1^+$ transition is forbidden via $E0$ decay as it would be in violation of the $\Delta N_{\text{phonon}} = \pm 0, 2$ selection rule. An estimation of $\rho^2(E0 : 0_2^+ \rightarrow 0_1^+) \times 10^3 = 27(1)$ can be made from

$$\rho^2(E0 : 0_2^+ \rightarrow 0_1^+) = \frac{2}{5} \frac{B(E2 \uparrow : 0_1^+ \rightarrow 2_1^+)^2}{(3/4\pi)^2 Z^2 r_0^8 A^{8/3}}, \quad (1)$$

^ae-mail: evitts@triumf.ca

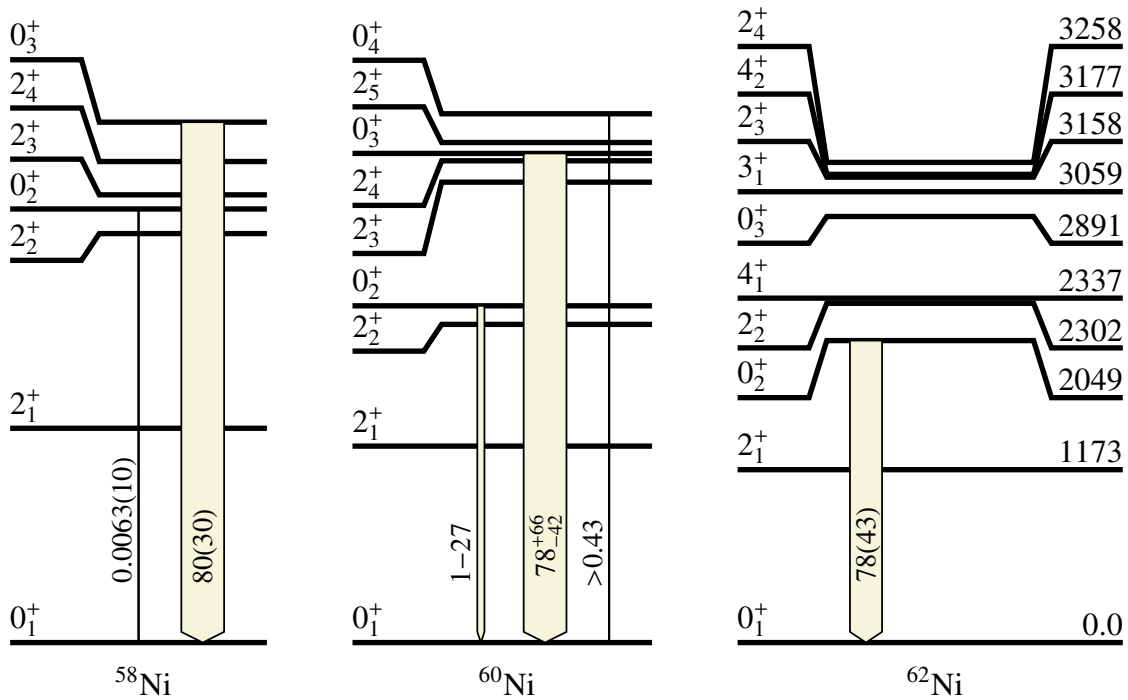


Figure 1. The low-lying states in $^{58,60,62}\text{Ni}$. Only the 0^+ and 2^+ states are shown for $^{58,60}\text{Ni}$. The previously measured $E0$ transitions, along with their associated strength, are shown by the arrows [5]. Note that only $0^+ \rightarrow 0^+$ transitions have been measured previously.

where Z is the atomic number, A is the mass number, r_0 is 1.3 fm and $B(E2)$ has units of $e^2 \text{ fm}^4$ [11]. If ^{62}Ni is a rigid rotor and the first 0^+ state is assumed to be a beta vibration, then the $\rho^2(E0) \times 10^3$ values between the beta band and the ground-state band (independent of angular momentum) are estimated to be 261(7) from

$$\begin{aligned} \rho^2(E0) &= \frac{9}{8\pi^2} Z^2 \beta_0^4 \frac{E(2_1^+)}{E(0_\beta^+)} \\ &= \frac{B(E2 : 0_1^+ \rightarrow 2_\beta^+) \uparrow 4\beta_0^2}{e^2 r_0^4 A^{4/3}}, \end{aligned} \quad (2)$$

where E is the energy, β refers to the beta band, e is the charge of the electron and β_0 is the quadrupole deformation [11].

2 Experiment

The 14UD Heavy Ion accelerator at the Australian National University was used to bombard an isotopically enriched ^{62}Ni target inside the Super-e electron spectrometer [12, 13] with a proton beam. A target and tuning aperture are available on a common actuator. The 5-mm diameter tuning aperture is coated with scintillating chromium-doped aluminium oxide. During beam tuning a light-sensitive camera is used to visualize the beam spot size and position. The second target position is the reaction target and it is tilted at 45 degrees to the beam axis, as shown in Fig. 2, such that the electrons and positrons are emitted towards the electron detectors through a smaller

effective target thickness and therefore experience less energy straggling.

The spectrometer operates using a solenoid magnet, with the central axis arranged perpendicular to the beam direction. Electrons from the target are guided to an array of six 9-mm thick lithium-drifted Silicon [Si(Li)] detectors which are located 350 mm away from the target and cooled with liquid nitrogen. The strength of the magnetic field of the solenoid is adjusted in order to select a momentum window for the transmission of a particular electron or positron energy. Two baffles and a diaphragm are located between the target and the detector, with the purpose of shielding the detectors from direct illumination of γ radiation from the target, and to prevent the transmission of low-energy electrons along the central axis. Electrons and positrons cross the central axis twice before reaching the detectors completing 2.5 helical orbits, as shown in the schematic of the spectrometer in Fig. 2. During normal operation, the magnetic field is swept back and forth between the minimum and maximum magnetic field values, covering the range of expected transition energies.

The relative efficiency of the HPGe detector was determined by the use of a ^{56}Co source. The relative efficiency of the Super-e spectrometer was determined by populating states in ^{54}Fe through inelastic proton scattering at 6.9 MeV and measuring the internal conversion coefficients of the pure $E2$ transitions that de-populate the excited states. Excited states in ^{62}Ni were populated through inelastic proton scattering of a 500-nA, 5-MeV proton beam incident on a 1.2-mg/cm² thick self-supporting ^{62}Ni target for a period of 24.5 hours.

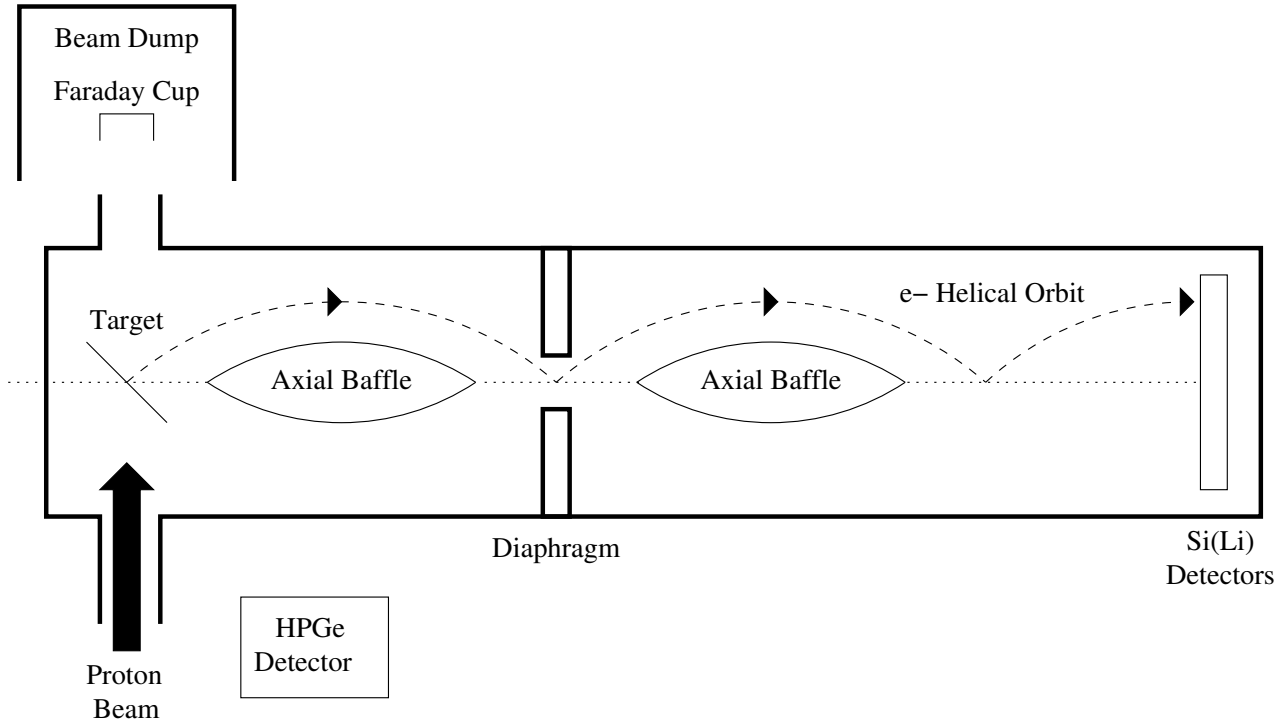


Figure 2. A schematic of the Super-e spectrometer. A proton beam is incident on a tilted target; the electrons are emitted outside of the rear and transported by the means of a solenoid magnet around two axial baffles and through a diaphragm onto an array of Si(Li) detectors.

3 Results

The spectrometer has a finite momentum acceptance window for each magnetic field setting. The signal-to-background ratio of the electron spectra can be improved if a software condition is imposed on the fraction of B to $B(\rho)$ in the event by event data. The momentum-window gated electron spectrum, along with the Ge singles, is shown in Fig. 3. The observed transitions in ^{62}Ni are shown by the dashed lines, the other transitions in the Ge singles are from the ^{63}Cu (p, γ) reaction. An excitation function was performed for beam energies between 5 and 6.5 MeV. A beam energy of 5 MeV was chosen in order to maximize the cross section for populating excited states in ^{62}Ni whilst keeping the cross section of the ^{63}Cu (p, γ) and ^{62}Cu ($p, n\gamma$) channels to a manageable level.

In order to validate the method of determining $\rho^2(E0)$ values and our understanding of the relative efficiencies, a q^2 value (i.e. the ratio of $E0$ to $E2$ electrons) of 0.088(5) was measured for the $0_2^+ \rightarrow 0_1^+$ transition in ^{62}Ni . The uncertainty in q^2 is calculated from the statistical uncertainty and systematic error in the efficiency of the Super-e detector. This value agrees within 1σ of the previously measured value of 0.084(11) [3, 5]. The mean lifetime, τ , of the 0_2^+ state at 2048.68 keV has been measured in a $^{59}\text{Co}(\alpha, p\gamma)$ reaction as $1.1^{+1.1}_{-0.4}$ ps [15], and in a $^{62}\text{Ni}(n, n'\gamma)$ reaction as $2.6^{+2.7}_{-0.9}$ ps [8]. Thus, the weighted average of the two data points was calculated to be $1.3^{+1.0}_{-0.3}$ ps. The $\rho^2(E0)$ value was determined to be $77^{+23}_{-34} \times 10^{-3}$ by using the mean-lifetime and

$$\rho^2(E0) = q_K^2 \times \frac{\alpha_K(E2)}{\Omega_K(E0)} \times W_\gamma(E2), \quad (3)$$

where Ω_K is the electronic factor and α_K and W_γ are the theoretical internal conversion coefficient [16] and partial decay constant of the $0_2^+ \rightarrow 2_1^+$ transition [5]. By utilizing similar methods, the $\rho^2(E0)$ value of the $2_2^+ \rightarrow 2_1^+$ was found to be roughly three times larger than the 0_2^+ to 0_1^+ transition. It was also possible in this experiment to place upper limits for the 0_3^+ to 0_1^+ and 0_3^+ to 0_2^+ transitions.

4 Summary

The $\rho^2(E0)$ values in ^{62}Ni for transitions between $J_i^\pi = J_f^\pi$ states were measured using the Super-e spectrometer at the Australian National University. The strength of the 0_2^+ to 0_1^+ transition was re-measured to be $77^{+23}_{-34} \times 10^{-3}$ and agrees with previously reported values. Upper limits have been placed on the 0_3^+ to 0_1^+ and 0_3^+ to 0_2^+ transitions. The measured $\rho^2(E0)$ value of the 2_2^+ to 2_1^+ transition in ^{62}Ni has been measured for the first time and found to be one of the largest $\rho^2(E0)$ values measured to date in nuclei heavier than Ca. This large value for the 2_2^+ to 2_1^+ transition can not be sufficiently explained by the simple harmonic quadrupole vibrational picture. The full results from this study will be presented in a future publication [17]. Similar investigations of $E0$ transition strengths between $J_i^\pi = J_f^\pi$ states in the other stable nickel isotopes are underway using the same experimental setup at the ANU.

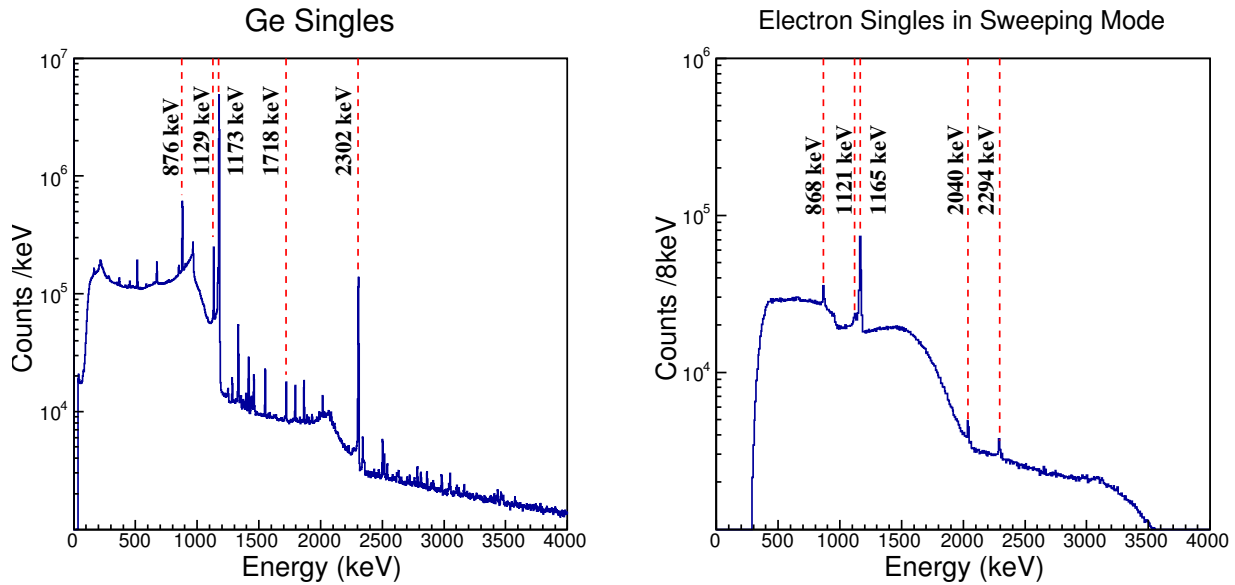


Figure 3. The energy spectra for (left) the Ge singles and (right) the electron singles in sweeping mode of the spectrometer, over the whole experimental run. The labelled peaks are the transitions observed from the de-exciting states in ^{62}Ni . In the electron spectrum, the K conversion electron peaks are highlighted, where the K-shell electron binding energy in Ni is 8.3 keV [14]

References

- [1] K. Heyde and J. Wood, *Rev. Mod. Phys.* **83**, 1467 (2011).
- [2] G. Ilie and R. F. Casten, *Phys. Rev. C* **84**, 064320 (2011).
- [3] A. Passoja *et al.*, *Nucl. Phys. A* **363**, 399 (1981).
- [4] E. K. Warburton and D. E. Alburger, *Phys. Lett. B* **36**, 38 (1971).
- [5] T. Kibédi and R. H. Spear, *Atomic Data and Nuclear Data Tables* **89**, 77 (2005).
- [6] J. M. G. Gómez, *Phys. Rev. C* **6**, 149 (1972).
- [7] N. J. Stone, *At. Data Nucl. Data Tables* **90**, 75 (2005).
- [8] A. Chakraborty *et al.*, *Phys. Rev. C* **83**, 034316 (2011).
- [9] P. E. Garrett *et al.*, *Phys. Rev. C* **78**, 044307 (2008).
- [10] P. E. Garrett and J. L. Wood, *J. Phys. G* **37**, 064028 (2010).
- [11] J. L. Wood *et al.*, *Nucl. Phys. A* **651**, 323-368 (1999).
- [12] T. Kibédi *et al.*, *Eur. Phys. J. Web Conf.* **35** 06001 (2012).
- [13] T. Kibédi *et al.*, in proceedings of “XII. International Symposium on Nuclei in the Cosmos”, PoS(NIC XII)203 (2012).
- [14] J. A. Bearden, *Rev. Mod. Phys.* **39**, 78 (1967).
- [15] D. L. Kennedy *et al.*, *Nucl. Phys. A* **308**, 14 (1978).
- [16] T. Kibédi *et al.*, *Nucl. Inst. and Meth. A* **589**, 202 (2008).
- [17] L. J. Evitts *et al.*, *to be published* (2016).